

# Using numerical weather prediction errors to estimate aerosol heating

By I. CARMONA\*, Y. J. KAUFMAN† and P. ALPERT, *Department of Geophysics and Planetary Sciences, Faculty of Exact Sciences, Tel Aviv University, Tel Aviv, 61390, Israel*

(Manuscript received 30 May 2007; in final form 5 June 2008)

## ABSTRACT

The total real response of the atmosphere to aerosols can be predicted by examining numerical models. In this study, the moderate resolution imaging spectroradiometer (MODIS) aerosol optical thickness (AOT) is correlated to model temperature errors to estimate this response for Israel and for Italy. Significant correlations between aerosols and atmospheric numerical model temperature errors are presented. Two main results were found in this study. First, the correlation between the UK Meteorological Office (UKMO) model temperature error ( $\Delta T$ ) at level 850 hPa for Tel Aviv (Israel) during the year 2002 and the MODIS AOT  $\geq 0.5$ , was found to be  $-0.54$ . Second, the sign of the correlation between the European Center for Medium-Range Weather Forecasting (ECMWF) monthly averaged model surface temperature errors for Italy and the MODIS AOT depends on the aerosol type, as reflected by the specific area. The correlation between air surface ECMWF  $\Delta T$  and AOT was found to be  $+0.70$  in southern Italy. Although the contribution of aerosols is ignored by most models, the findings presented here are statistically significant and provide a first reliable estimation of the realistic full atmospheric temperature response to aerosol processes.

## 1. Introduction

Aerosols have various effects on the atmospheric energy balance, often categorized as direct (radiative response), indirect (cloud interaction) or semi-direct (e.g. cloud and boundary layer interactions). These effects are not usually incorporated in current operational numerical weather prediction models for several reasons. This is probably due, primarily, to the fact that the precise 3-D distribution of aerosols is not known well enough to allow realistic model initialization (Alpert et al., 2002). In addition, the physical/chemical effects of aerosols on the atmospheric energy balance, and in particular, their various interactions with clouds are not well constrained (Ramanathan et al., 2001; Kaufman et al., 2002). Jacobson and Kaufman (2006) have shown that model sensitivity studies with and without aerosols are useful in estimating the atmospheric response to aerosols. Some operational models do include monthly-averaged patterns of aerosols in their radiative calculations but certainly not realistic daily distributions (Tanré et al., 2001). The contribution of aerosols in climate models is estimated to be non-negligible but, at the same time, carries high uncertainties (IPCC, 2001).

This study quantifies aerosol-related temperature errors in numerical weather prediction (NWP) models, for different regions under specific synoptic conditions. This was achieved by employing aerosol data from the moderate resolution imaging spectroradiometer (MODIS), in conjunction with data on model errors available from operational NWP centres. This idea was first explored by Alpert et al. (1998, 2000) for climate modelling; however, here it is a first attempt to employ this method on NWP models.

For the most part, the effects of dust on temperature were studied. Other types of aerosols were also examined, such as, anthropogenic aerosols from urban and industrial pollution. In the Eastern Mediterranean, there are three major types of aerosols:

(1) Sulphate aerosols that are emitted from industrial activity in the region or are carried by northwesterly winds from Europe. Most of these aerosols can be found in the 1000–850 hPa layer (Wanger et al., 2000).

(2) Mineral dust that is blown from North Africa to southern Europe, the Eastern Mediterranean and even to the east coast of the USA. The dust plumes are mostly found at the 850–400 hPa layer. Figure 1 shows, for example, predicted aerosol concentrations for the forecast time of +24 h in Tel Aviv during the year 2002, for days with MODIS aerosol optical thickness (AOT) equal or greater than 0.5. About 70% of the dust mass is concentrated in the 850–400 hPa layer, according to the predicted vertical profile of aerosol concentration using the ETA

\*Corresponding author.  
e-mail: isaaccar@post.tau.ac.il  
†Deceased, NASA/GSFC.  
DOI: 10.1111/j.1600-0889.2008.00371.x

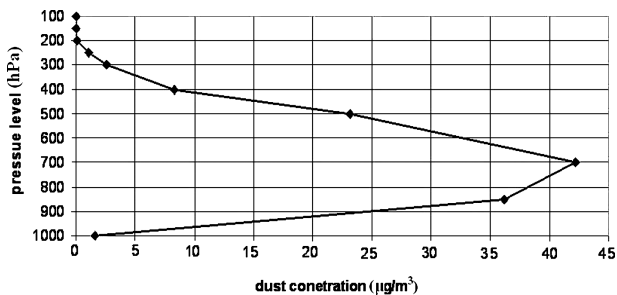


Fig. 1. Predicted mineral dust aerosol concentration ( $\mu\text{g m}^{-3}$ ) for 2002, by the dust prediction ETA model for cases with aerosol optical thickness (AOT)  $\geq 0.5$ , based on MODIS TERRA for gridpoint ( $32.0^\circ\text{N}, 35.0^\circ\text{E}$ ). Predicted time is 12 UTC, forecast running time is for 24 h.

model at Tel Aviv University. ETA is a numerical weather model that, among its other applications, also predicts dust concentrations for aerosols with a representative mode size of  $2.5 \mu\text{m}$ . The maximum forecast time of ETA is 48 h, and it starts prediction from 12 UTC. ETA's resulting grid resolution is  $0.5^\circ$  for latitude and longitude, and its vertical distribution is 10 pressure levels between 1000 and 100 hPa. ETA started to produce forecast data from January 2001 (Alpert et al., 2002, 2004).

(3) Mineral dust that is blown from the Saudi deserts and is common in synoptic systems such as the Red Sea trough, with typical winds from the easterly sector (Erel et al., 2006). The average number of days per year that the AOT for the  $0.55 \mu\text{m}$  wavelength is larger or equal to 0.5 is 60–70 d. This number is based on Terra satellite AOT (Sec. 3) observations averaged for 2000–2004.

Dust storms are frequent in March–May and September–November, occurring during the Sharav cyclones that bring spring air masses from North Africa (Alpert and Ziv, 1989). However, mineral dust can also be found in other synoptic systems, such as the Cyprus low during winter and during summer.

In 2002, for the Tel Aviv gridpoint and based on MODIS Terra data, 44 d were found with AOT larger or equal to 0.5, as well as the available UK Meteorological Office (UKMO) model temperature error ( $\Delta T$ ) at 12 UTC. In this study, a day with dust storm is defined as a day with AOT larger or equal to 0.5. Figure 1 presents the vertical profile for an average mineral dust aerosol over a gridpoint near Tel Aviv, during dust storms in 2002. The figure shows the dust concentration ( $\mu\text{g m}^{-3}$ ) profile predicted at 12 UTC from the ETA forecast model at Tel Aviv University. Forecast period is 24 h. It can clearly be seen that on the average, about 87% of the dust mass is found above 850 hPa. The majority of the dust mass (94%) is located beneath 400 hPa. Hence, according to the model distribution, 13% of the dust mass is located between 1000–850 hPa, and 65% of the dust mass is in the 850–500 hPa layer.

The main objective of this study is to investigate the model temperature error,  $\Delta T$ , caused by aerosols at different altitudes

and to examine the relationship between the altitude of maximum aerosols and that of maximum  $\Delta T$ . This study will also evaluate the effects of various types of aerosols, such as mineral dust and anthropogenic sulphates from air pollution, on numerical weather prediction errors. The focus will be given here to temperature since it is a variable quite accurately estimated in atmospheric model analysis (in contrast to rainfall, where the standard deviation of the model error can be in the order of the predicted amount of rain or even larger).

## 2. Data and models

### 2.1. MODIS data

MODIS data from the internet, which provides a global data set of AOT for the 550 nm wavelength, were used in this study to quantify atmospheric AOT. This data has a spatial horizontal resolution of  $1^\circ \times 1^\circ$ . Above the Sahara desert reliable data is not available due to the high surface reflection of visible radiation. In areas with high albedo, the accuracy of the data is low (Kaufman et al., 2002), whereas above water bodies it is high. Our study will include the following two sets of AOT data:

*2.1.1. Monthly mean AOT.* Monthly data of Terra include AOT (coarse and fine particles), coarse AOT (particle radius 1–20  $\mu\text{m}$ ), fine AOT (particle radius 0.1–1  $\mu\text{m}$ ) and the aerosol fine mode fraction ('f'), which is the fraction of AOT caused by fine particles with a radius of less than 1  $\mu\text{m}$  (MOVAS, 2007a). The data set begins on March 2000.

*2.1.2. Daily AOT.* Daily data of Terra AOT (MOVIS, 2007b) for fine and coarse particles are of the same resolution as the monthly data. This data set also runs from March 2000. Observations are recorded daily in the morning, but the time varies due to the fact that the satellite does not complete a full orbit every 24 h. Terra was launched in a near polar orbit, descending southward every day at 10:30 am equator crossing time (Xiong et al., 2003). Therefore, it is observed almost every day at every gridpoint, at around 10:30 am local time (LST), as the satellite is at its maximum inclination in the sky.

### 2.2. ETA model

This model, as described in Section 1, provides predicted vertical profiles of aerosol concentration to complement the horizontal AOT maps provided by the satellite. Predicted data for dust concentration was employed as opposed to measured data, seeing as retrieval of dust vertical profiles is not accurate as discussed in Alpert et al. (2002).

### 2.3. UKMO data

The UKMO model was used to evaluate temperature model errors above Tel Aviv at the 850 hPa pressure level. Daily

information from the model is available at 00 UTC and 12 UTC. The global model has a longitudinal spatial resolution of  $0.8333^\circ$ , a latitudinal resolution of  $0.5555^\circ$  (approximately 60 km) and contains 38 vertical pressure levels. The UKMO is using the ensemble forecasting method for its model initialization (Met. Office website: <http://www.metoffice.gov.uk/research/nwp/ensemble>).

The UKMO model output has the relevant pressure levels in the 1000–500 hPa layer employed here and contains atmospheric variables that are relevant for this study, such as temperature, clouds, precipitation, winds, humidity, etc. However, this model lacks information on aerosol prediction.

#### 2.4. European Centre for Medium-Range Weather Forecasts (ECMWF)

The ECMWF model output in this study was used to evaluate ground surface temperature model errors over Italy. ECMWF is a global model with available predictions in Israel up to +144 h. The model resolution employed here was  $2^\circ \times 2.5^\circ$ . The ECMWF initial condition is based on ensemble prediction system (EPS), which runs the model 51 times. Each run is slightly different in its initial condition (perturbation). The perturbations are designed to represent the uncertainties in the forecast results in the operational prediction (Buizza et al., 2003; ECMWF, 2002). In this study, surface temperatures were analysed in Italy for a forecast time of +12 h.

#### 2.5. MM5 (Tel Aviv University Mesoscale Model)

The MM5 model in this study was used to evaluate ground surface model temperature errors over the Eastern Mediterranean. The MM5 is a mesoscale model that runs twice daily, for +54 h at the Tel Aviv University (TAU) Weather Research Center (TAU-WERC, 2007). Initial conditions for MM5 are provided by the National Center for Atmospheric Research (NCAR) or by UKMO. The operational archive covers the period from January 2001 to the present. Data forecast times were +12 h, +24 h, +36 and +48 h with three-hour intervals. A description of the model version used at TAU can be found in Krichak et al. (2007).

### 3. Methodology

#### 3.1. Tel Aviv analysis

A correlation between daily observations of MODIS AOT and  $\Delta T$  for the UKMO model was employed in the analysis for the Tel Aviv area. As explained, AOT data from the Terra satellite corresponded to measurements in the morning at around 10:30 LST, which is 8:30 UTC at Tel Aviv.  $\Delta T$  was defined as the temperature difference between that observed at the Bet Dagan station (meteorological station number 40179, 12 UTC radiosonde) and the UKMO predicted temperature at +12 h,

+24 h and +36 h forecasts; all predicted for 12 UTC. The error due to the time difference for aerosol data of about 3.5 h, was assumed small. The UKMO forecast temperature at Bet Dagan (approximately  $32.0^\circ\text{N}$ ,  $35.0^\circ\text{E}$ ) was calculated by linear interpolation of the nearest four gridpoints. Resolution of UKMO forecasts were  $0.56^\circ \times 0.83^\circ$ . As stated, data for 2002 were analysed.

#### 3.2. Italy analysis

For the Italian region, the correlation between monthly available mean  $\Delta T$  and monthly mean AOT, was employed. The country was divided into three areas: southern, central and northern Italy. Mean  $\Delta T$  was defined as the area average of the monthly  $\Delta T$  for all meteorological stations. For each meteorological station, the monthly mean of  $\Delta T$  was calculated as the monthly average of all daily observed  $\Delta T$  from the ECMWF model. The  $\Delta T$  of each station was calculated as station observed temperature at 12 UTC minus the ECMWF predicted temperature at this hour with a forecast time of +12 h. The predicted temperature for each station was found after interpolation from model gridpoints to the station. Temperature of the gridpoints was predicted for a pressure level of 1000 hPa. Table 1 presents the list of meteorological station numbers for each area (southern, central and northern Italy).

Mean AOT was calculated as the monthly mean value observed by the Terra satellite. In Italy, Terra AOT is observed 1 h earlier than in Israel. Hence, the total time difference is of about 2.5 h, and its associated error is neglected.

Table 2 presents details about the geographical latitude range that was used for each area in Italy for the AOT calculation.

Observed temperature was taken from meteorological stations and model temperature was interpolated from model gridpoints to station.  $\Delta T$  and AOT monthly means were analysed for the period of January 2001 to April 2002. This period contains 15 pairs of monthly averages ( $\Delta T$  for October 2001 was absent). The remaining months of 2002 were not included in the analysis because during this period,  $\Delta T$  abruptly increased by 1–2 K due to a change in the modelling system (M. Colacino, personal communication, 2003).

#### 3.3. AOT and $\Delta T$ lag

**3.3.1. The lag hypothesis between AOT and  $\Delta T$ .** In the third and last part of this study, the correlation between a fixed  $\Delta T$  gridpoint and the surrounding AOT gridpoints were examined. The purpose was to show that on a horizontal or constant pressure correlation map between a fixed  $\Delta T$  gridpoint (in our case Tel Aviv, Israel) and surrounding AOT gridpoints, maximum correlation is not necessarily located at the fixed gridpoint but at some distance from it. This distance, termed here 'lag', is approximated by the average horizontal wind velocity in this area multiplied by the model forecast time (the forecast time used to

Table 1. Meteorological stations in Italy

Southern Italy	Central Italy	Northern Italy
16289 NAPLES	16181 PERUGIA	16044 UDINE
16320 BRINDISI	16191 ANCONA	16059 TURIN
16429 TRAPANI/BIRGI <sup>a</sup>	16230 ROME	16080 MILANO/LINATE
16480 COZO SPADARO <sup>a</sup>	16245 PRATICA DI MARE	16120 GENOA
	16520 ALGHERO <sup>b</sup>	16140 BOLOGNA
	16560 CAGLIARI/ELMAS <sup>b</sup>	16158 PISA/S. GIUSTO

<sup>a</sup>Stations in Sicily.

<sup>b</sup>Central Italy contains two regions: the land itself and Sardinia.

Table 2. Geographical latitudinal ranges for each area in Italy

Southern Italy	Central Italy <sup>a</sup>	Northern Italy
37°N–41°N, 12°E–17°E	(1) 41°N–43.5°N, 12°E–13.5°E (2) 39°N–41°N, 8E–9°E (Inland)	43.5°N–47°N, 8°E–13°E

<sup>a</sup>Central Italy contains two regions: the land itself and Sardinia.

define  $\Delta T$ ). This lag hypothesis was tested only in Tel Aviv. The physical explanation for this lag follows.

It is expected that errors in  $\Delta T$  will gradually develop from the initiation time of the model, until the end of the run (forecast time). However, dust in the forecasting time period is generally not stationary but moves with the wind. During its journey, air temperature may be affected by aerosols, which generate heating or cooling. Hence, a model that does not take into account the effect of these aerosols will exhibit an error in  $\Delta T$ . Air motion will cause a lag in the correlation between AOT and  $\Delta T$ . This means, for instance, that the maximum correlation between AOT and  $\Delta T$  may be expected near levels of maximum dust concentration but not in the same location. It is important to note that though the aerosol effects are not part of the NWP model simulations, the simulations are initiated using the observed meteorological conditions at the start of the run, which implicitly include any aerosol effects on those conditions given the aerosol distribution at that time.

**3.3.2. The method for finding the lag correlation in the East Mediterranean.** Maximum correlation between Tel Aviv MM5  $\Delta T$  and MODIS Terra AOT at each gridpoint over the geographical area 27.5°N–37.5°N, 29.5°E–40.5°E, was examined for a rectangle of 11 × 12 gridpoints or 132 MODIS gridpoints. The correlation calculation was performed for Tel Aviv  $\Delta T$  pressure levels 1000, 850, 700 and 500 hPa, where most of the dust mass layer is concentrated (Fig. 1).  $\Delta T$  was defined as the MM5 analysis temperature for the MM5 gridpoint (32.64°N, 35.18°E), close to Tel Aviv, minus the predicted temperature for this hour and with a forecast time of 12 h. Correlation was found between a stationary gridpoint  $\Delta T$  and spatial gridpoints of AOT that

were not taken from the same location. The correlation is based on the daily data from April 2001 to April 2005 (2003 is absent). Each correlation gridpoint in the map (Fig. 4) is based on about 54–92 observations. Two types of correlation were calculated; one for  $\Delta T + 12$  h and the second for  $\Delta T + 24$  h. The lag is the distance between the model  $\Delta T$  gridpoint to the point of maximum correlation with AOT. The hypothesis is that there, is a lag equal to the forecast time, multiplied by mean wind velocity at the pertinent pressure level. This lag is independent upon the dust mass, travelling during the forecast time over a given distance. The model temperature errors, defined here at the MM5 Tel Aviv gridpoint, gradually increase during forecast time, and hence  $\Delta T$  is far from the point of maximum correlation, by a distance that is about equal to the velocity of wind multiplied by the forecast time. In addition, the azimuth of  $\Delta T$  from the point of maximum correlation is expected to correspond to wind direction. For example, if the wind was blowing from west to east, the point of maximum correlation is expected to be located west of the  $\Delta T$  location.

## 4. Results

### 4.1. Tel Aviv analyses

**4.1.1. Correlations between  $\Delta T$  and high AOT ( $AOT \geq 0.5$ ) in 2002.** The correlation between the 850 hPa UKMO output  $\Delta T$  and the MODIS AOT for a wavelength of 0.55  $\mu\text{m}$  was found to be as much as  $-0.54$  during the year 2002 (Table 3). This correlation was obtained for 44 cases with  $AOT \geq 0.5$  (for  $AOT < 0.5$ , see Section 4.1.2). An extreme AOT point,  $AOT = 1.1$ , was found on the 16 April 2002.

Table 3. Correlation between  $\Delta T$  at level 850 hPa and AOT in Tel Aviv, during 2002. The slope coefficient ( $b$ ) is based on the linear regression:  $\Delta T = a \pm b^a \text{AOT}$

Forecast time (h)	AOT	Correlation	Significance level (%) of correlation based on $t$ -test <sup>a</sup> ( <sup>b</sup> Bootstrap)	Slope coefficient ( $b$ ) [K/AOT]	Standard deviation of the slope coefficient ( $\sigma_b$ ) [K/AOT]	Significance level (%) of correlation from $t$ -test <sup>a</sup> ( <sup>b</sup> Bootstrap)	Number of observations
12	AOT < 0.5	0.05	50.7	0.40	0.60	50.3	210
	AOT $\geq$ 0.5	<b>-0.54</b>	<1 (0.01)	<b>-5.21</b>	1.27	0.02 (0.02)	44
24	AOT < 0.5	0.13	5.71	1.36	0.71	5.7	209
	AOT $\geq$ 0.5	<b>-0.50</b>	<1 (0.06)	<b>-5.74</b>	1.57	0.07 (0.01)	43
36	AOT < 0.5	0.11	11.5	1.22	0.79	12.7	207
	AOT $\geq$ 0.5	<b>-0.45</b>	<1 (0.01)	<b>-5.72</b>	1.73	0.19 (0.01)	46

<sup>a</sup>T-test with the assumption of normal distribution.

<sup>b</sup>Bootstrap results are based on 10000 computer calculation loops.

Numbers in bold mean that significant level higher than 5% ( $p < 5\%$ ).

After removing this point from the calculation, a significant negative correlation of  $-0.39$  ( $p = 1\%$ ) was still found. The UKMO forecast time employed was +12 h and the predicted time was 12 UTC. The negative correlation suggests significant cooling at 850 hPa ( $\sim 1.5$  km above sea level) when AOT is equal to, or above, 0.5. The significance level was calculated by the bootstrap method, which does not assume that data have a normal distribution.

For other levels such as 500 hPa and surface levels (2 m), the correlation was below  $-0.2$ . For a forecast time of +24 h, the correlation dropped slightly to  $-0.49$ . This reduction suggests that for longer forecasting times, model temperature errors caused by other atmospheric processes increase relative to the effect of aerosols. For +48 h, the correlation was further reduced to  $-0.45$ . Moreover, in the above case (AOT  $\geq 0.5$ ) the total cloud fraction (from MODIS data) was somewhat higher by almost 0.1 (0.3 for AOT  $\geq 0$  and 0.4 for AOT  $\geq 0.5$ ). This may suggest that cases involving aerosols are associated with increased cloudiness and stresses the importance of aerosol–cloud interactions. Note that these cases occur primarily in the summer season in Israel, which, for the most part, is not characterized by significant cloudiness but by dry air in all tropospheric layers above pressure level 900 hPa (about 1000 m above sea level). During the summer, most clouds in Israel are fair-weather cumulus, with tops below 850 hPa. This is due to the height of the marine inversion, which is of the order of 1000 m above sea level. It is because of this that  $\Delta T$  at 850 hPa is not directly influenced by cloud–aerosol interactions. However, there is probably some increase in cloud amounts in the mixed layer due to the increase of aerosols. Results of a total cloud fraction (tcf) of 0.3 for AOT  $\geq 0$  and tcf = 0.4 for AOT  $\geq 0.5$ , with a high significance level ( $p < 5\%$ ), support this conclusion and also suggest that the interaction of aerosols with clouds cannot be ruled out as influencing  $\Delta T$ . It should be noted that for AOT less than 0.5, correlations between AOT and  $\Delta T + 12$  h,  $\Delta T + 24$  h and  $\Delta T + 36$  h are very low, that is, 0.05, 0.13 and 0.11, respectively.

4.1.2. *The large difference between high and low AOT.* Table 3 summarizes correlations between low AOT (AOT < 0.5) and high AOT (AOT  $\geq 0.5$ ), for forecasting times of +12, +24 and +36 h, during 2002. The slope coefficients ( $b$ ) of the linear regression ( $\Delta T = b^* \text{AOT} + a$ ), are also shown. The correlation is negative and high ( $>|-0.45|$ ) for high AOT, but for low AOT, the correlation for a forecasting time of +12 h becomes insignificant ( $p > 0.40$ ). In addition, the significance levels for forecasting times of +24 and +36 h are 6 and 11%, respectively.

Figure 2 shows scatter plots of  $\Delta T$  vs. AOT calculated for 850 hPa in Tel Aviv, during 2002. For the slopes of high AOT (AOT  $\geq 0.5$ ), linear regression exhibits a negative slope of approximately  $-5.21$  K/AOT, with relatively low variability (standard deviation of 1.27 K/AOT and  $p < 5\%$ ). However, the slopes for low AOT (AOT < 0.5), for a forecasting time of +12 h, are positive and, as expected, insignificant ( $p > 50\%$ ). Also, the standard deviation for low AOT is high. Hence, a significant cooling effect was found only for high AOTs.

Excluding the extreme point (AOT = 1.1 on 16 Apr 2002 discussed in Section 4.1.1) from the linear regression does not change the sign of the effect (from cooling to heating). In this case, the linear regression calculation gives a negative AOT coefficient of  $-4$  with relatively small variability, a standard deviation of 1 K/AOT and a high significance level ( $<2\%$ ).

It is interesting to note the sensitivity of our results to the threshold AOT = 0.5. If one chooses a higher threshold of AOT = 0.7, for instance, the correlation increases to  $-0.76$ ,  $-0.71$  and  $-0.60$ , corresponding to forecast time of +12, +24 h and +36 h, respectively. And the slope of the curve becomes sharper, that is,  $-7.2$  with a standard deviation of 3.2 K/AOT and high significance level ( $p < 5\%$ ). In spite of the large drop in the number of points (9–10), the slope remains highly significant. Similar results are obtained for a threshold of AOT = 0.6 with 22–23 points.

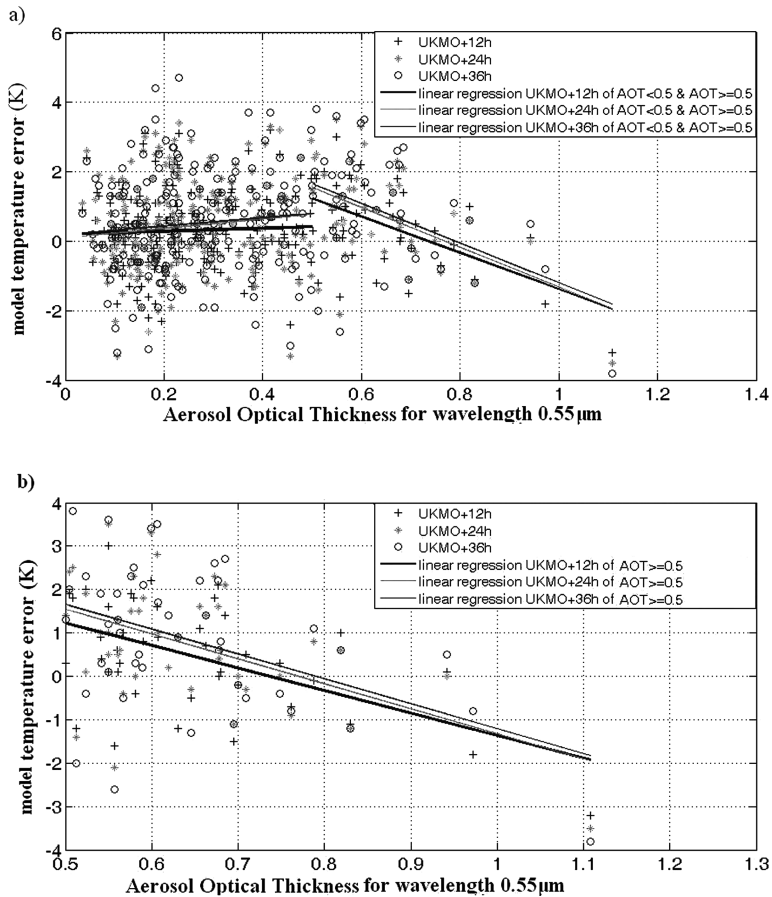


Fig. 2. Scatter plot (a) of noon data (12 UTC) for the year 2002 from Tel Aviv 850 hPa. Model temperature error,  $\Delta T$  (K) is defined as the radiosonde temperature observation minus UKMO high resolution model predicted temperature as function of MODIS Terra aerosol optical thickness (AOT). The points ('+') indicate  $\Delta T$  for forecast time of +12 h. Points ('\*') for  $\Delta T$  forecast time of +24 h and points ('o') for  $\Delta T$  forecast time of +36 h. The regression lines are divided into two parts: for aerosol optical thickness (AOT) < 0.5 & AOT  $\geq$  0.5. Scatter plot (b) is the zoom of plot (a) for AOT  $\geq$  0.5.

4.1.3. *The effect of changes in insolation on  $\Delta T$  and on AOT.* The seasonal change in insolation might also influence  $\Delta T$ <sup>1</sup>. Linear multiregression calculations were performed to separate the influences of both AOT and of daily solar radiation, on  $\Delta T$ .

We define solar variation parameter (svp) as a variable, which obtained a maximum value of 93 on 21 June 2002 (the longest day of the year) and a minimum value of 89 on 21 December 2002 (the shortest day of the year). The svp counts the days in this way. An assumption that the average daily mean radiation (incoming solar radiation at top of the atmosphere) changed linearly with the number of days, was made. Indeed, the change during the time of mean daily radiation behaved like a sine function. However, this change is slow. The results, which were derived by linear multiregression, suggest that the seasonal effect of svp on  $\Delta T$  is smaller than the aerosol effect. The assumption that svp has a sine functional change, was also examined and provided very similar results to the assumption of a linear change presented here.

Correlation between svp and  $\Delta T$  (+12 h) was found to be 0.24 but insignificant ( $p > 10\%$ ). This correlation is much lower in its absolute value than the correlation between AOT and  $\Delta T$

(−0.54). It is important to note that the two variables, AOT and svp, are only weakly interdependent; their correlation is 0.21 and  $p > 15\%$ .

Another comparison between the influence of AOT and svp can be made between slope coefficients. The svp coefficient is 0.014, with a standard deviation of 0.005 ( $p < 5\%$ ), whereas the high AOT aerosol coefficient is −5.96 K/AOT, with a standard deviation of 1.20 K/AOT ( $p < 5\%$ ). However, a direct comparison between these two coefficients is not valid because they have different units. Table 4 summarizes the correlations and the linear coefficients for the multiregression.

Multilinear regression shows that the average influence of the variable high AOT (AOT  $\geq$  0.5) on  $\Delta T$  is  $-3.84 \pm 0.77$  K, compared with the svp on  $\Delta T$ , which is only  $0.23 \pm 0.16$  K. Hence, the seasonal effect on model temperature errors is an order of magnitude smaller than the aerosol effect for daily Tel Aviv error predictions ( $p < 5\%$ ). In Italy, however, with monthly averages, the seasonal effect becomes significant, as shown in Section 4.2.

#### 4.2. Italy analyses

Correlations between southern and central Italy were found to be high but with opposing signs. Correlation for monthly means

<sup>1</sup>The idea, suggested by co-author Y K, was to eliminate the potential contribution of seasonal variations in solar heating on the  $\Delta T$  error.

Table 4. Multi linear regression of  $\Delta T$  as a function of aerosols (AOT) and of seasonality ('svp') during January 2001–March 2002 ( $\pm$  standard deviation)

	Southern Italy	Central Italy
Intercept [K]	<b>0.66 <math>\pm</math> 0.35<sup>a</sup></b>	0.05 $\pm$ 0.54
AOT coefficient [K/AOT]	-0.33 $\pm$ 2.37	-0.01 $\pm$ 4.48
'svp' coefficient [K/svp]	<b>0.25 <math>\pm</math> 0.12<sup>a</sup></b>	-0.21 $\pm$ 0.23

<sup>a</sup>Only in southern Italy the intercept and 'svp' coefficient have significant levels between 5 and 10% (8 and 6% for intercept and 'svp' coefficient respectively). All other values that are not marked are insignificant in 10% level.

(over 15 months from January 2001 to March 2002) between surface air  $\Delta T$  and AOT is as high as +0.70 for southern Italy and -0.72 for central Italy (Fig. 3, central Italy). Predicted temperature fields were taken from ECMWF-model surface data, model temperature errors for a forecast time of +12 h and the predicted time at 12 UTC. The linear regression coefficient of AOT, when considering only its effect in southern Italy, was found to be 4.06  $\pm$  1.16 and -4.06  $\pm$  1.09 K/AOT in central Italy. The intercept in southern Italy was -0.23 K  $\pm$  0.32 K and in central Italy -0.48 K  $\pm$  0.29 K. In southern and central Italy, the coefficients have a high significance level ( $p < 5\%$ ). However, the intercept values are not significant.

Although  $\Delta T$  to AOT correlations are high, it is probable that seasonality is a large contributor. Indeed, multiregression performed with both AOT and seasonality indicates a strong contribution of the latter. It seems, therefore, that monthly means may not be a good choice to detect aerosol signals, using the present methodology. Hence, it is planned to investigate daily

data from Italy for a specific season, such as summer during which the seasonality contribution is expected to be reduced. This may also be the reason why daily data from Tel Aviv revealed an insignificant contribution of seasonality, when based on the summer period only. Alternatively, a significant increase in the number of monthly data points for each season separately may also allow the elimination of the seasonality factor. The latter option is not so realistic because the prediction systems are often changed. Other potential reasons to explain the difference in the seasonality factor between the Tel Aviv case study and that of Italy are:

(1) The Tel Aviv case study is based on one station whereas the Italy case study is based on area averages, where the aerosol effect is strongly smoothed out.

(2) The model  $\Delta T$  in Tel Aviv was for level 850 hPa, whereas for Italy, it was taken at surface level. In addition, air near the ground is strongly influenced by other near-surface effects that obscure the aerosol signal.

Table 4 summarizes multilinear regression coefficients of  $\Delta T$  as function of both AOT and svp (see Section 4.1.3). Multilinear regression over southern Italy shows that the average influence of the variable 'high AOT' (AOT  $\geq$  0.5) on  $\Delta T$  is -0.08  $\pm$  0.03 K, compared with the seasonal effect (svp) on  $\Delta T$ , which is 0.71  $\pm$  0.44 K. Multilinear regression over northern Italy also shows that the average influence of high AOT on  $\Delta T$  is small, that is, 0.003  $\pm$  0.001 K, compared with the seasonal effect on  $\Delta T$ , which is -0.60  $\pm$  0.37 K.

Hence, over both southern and central Italy, the seasonality effect is predominant. These final results for the monthly average analysis show that the seasonal factor has more influence on model temperature errors than the AOT factor. Further discussion of these results is given in Section 6.

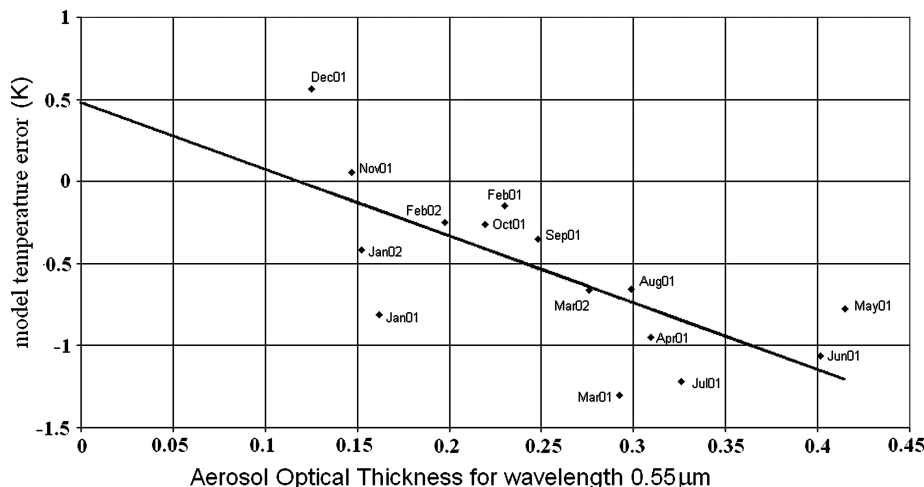


Fig. 3. Model temperature error (in K; observed temperature minus ECMWF temperature prediction to 24 h after interpolation to the station coordinate) vs. MODIS Terra aerosol optical thickness (AOT) in central Italy during January 2001–March 2002.

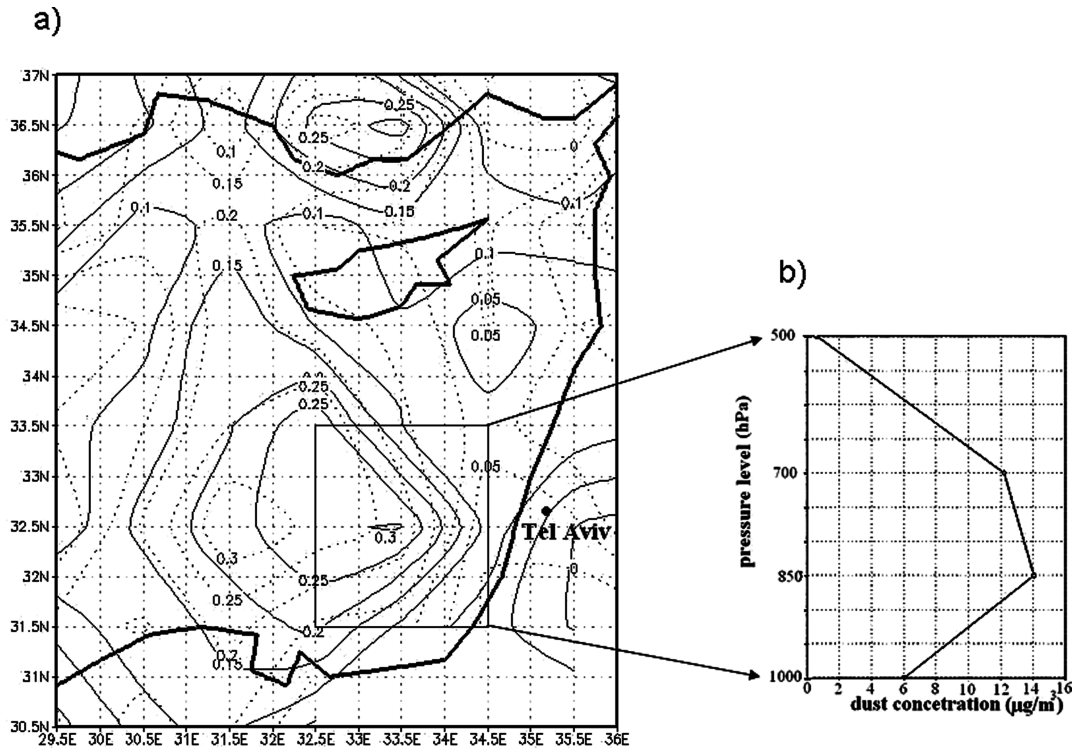


Fig. 4. Correlation map (a) between 700 hPa model temperature error,  $\Delta T$  (K) at Tel Aviv ( $32.64^{\circ}\text{N}$ ,  $35.28^{\circ}\text{E}$ ) and Aerosol Optical thickness (AOT) over the East Mediterranean MODIS Terra gridpoints (see Section 2.1). The correlation is for April 2001, 2002, 2004 & 2005 for noon observations (12 UTC). Solid contour lines are for  $\Delta T$  (+12 h) and the dashed lines are for  $\Delta T$  (+24 h).  $\Delta T = (\text{MM5 analysis } 12 \text{ UTC}) - (\text{MM5} + \text{forecast hours})$ . Panel (b) shows the average vertical profile of dust based on ETA output ( $T + 24$  h) over the region of maximum correlation indicated by the square in (a).

### 4.3. Lagged correlations between $\Delta T$ and AOT—Eastern Mediterranean

**4.3.1. Temporal changes in the maximum correlated area.**  $\Delta T$  correlation maps for levels 1000, 850 and 500 hPa do not show a significant correlation in the Mediterranean Sea. The maximum correlations in these maps are lower than 0.2, and because there are only 60–90 observations, the correlation does not reach the significant level of 5%. Only at the 700 hPa level (Fig. 4), does the map's maximum correlation, 0.3 for  $\Delta T$  (+12 h), become significant. This correlation is based on 60 observations with a 5% significance. This point of maximum correlation (Fig. 4, the dashed contours) is located at the grid-point  $32.5^{\circ}\text{N}$ ,  $32.5^{\circ}\text{E}$ , which is approximately 200 km west of Tel Aviv. Maximum correlation between MODIS AOT and 700 hPa  $\Delta T$  (+24 h) is of the same magnitude as in the  $\Delta T$  (+12 h) map, but the maximum is, as expected, further west by  $\sim 200$  km (Fig. 4, the dashed contours). The maximum correlation is located at  $32.5^{\circ}\text{N}$ ,  $30.5^{\circ}\text{E}$  and is approximately 400 km west of Tel Aviv. The value of maximum correlation is 0.34 and is based on 61 observations with 5% significance.

**4.3.2. The shift of the maximum correlation pattern.** Figure 5 shows the horizontal and vertical shift of the maximum cor-

relation over a latitudinal cross-section at  $32.5^{\circ}\text{N}$ . It presents the longitudinal, as well as the vertical movement, of the point of maximum correlation. The shaded area represents correlations between Tel Aviv  $\Delta T$  (+24 h) and each gridpoint of AOT, whereas the line contours represent correlation for  $\Delta T$  (+12 h). The shift of the point of maximum correlation as  $\Delta T$  forecast time becomes shorter, is evident. However, concurrently, the area of correlation is expanded higher, suggesting that dust is lifted up as it moves east (as discussed earlier), explaining the 700 hPa wind intensity. This might explain why the calculated wind (theoretical wind) is lower than the actual (statistical) wind measured at 700 hPa. Dust at the Tel Aviv gridpoints at 700 hPa probably originated from lower heights as it came from west of Tel Aviv. Alpert et al. (2004) illustrated the significant upward motion of dust as it moves over the Mediterranean from the Sahara.

Figure 6 shows the vertical profile of dust concentration predicted by the ETA model for +24 h. Most of the dust mass is located at the 700 hPa level, where the maximum correlation along the vertical axis is also found. The positive correlation indicates warming due to aerosols, which reaches a maximum at the upper section of the dust layer.



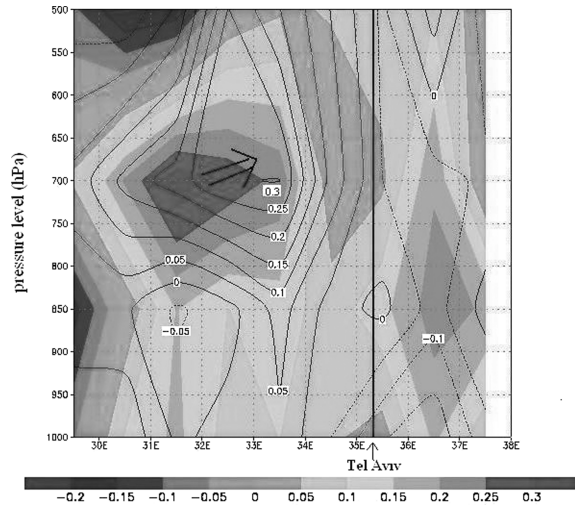
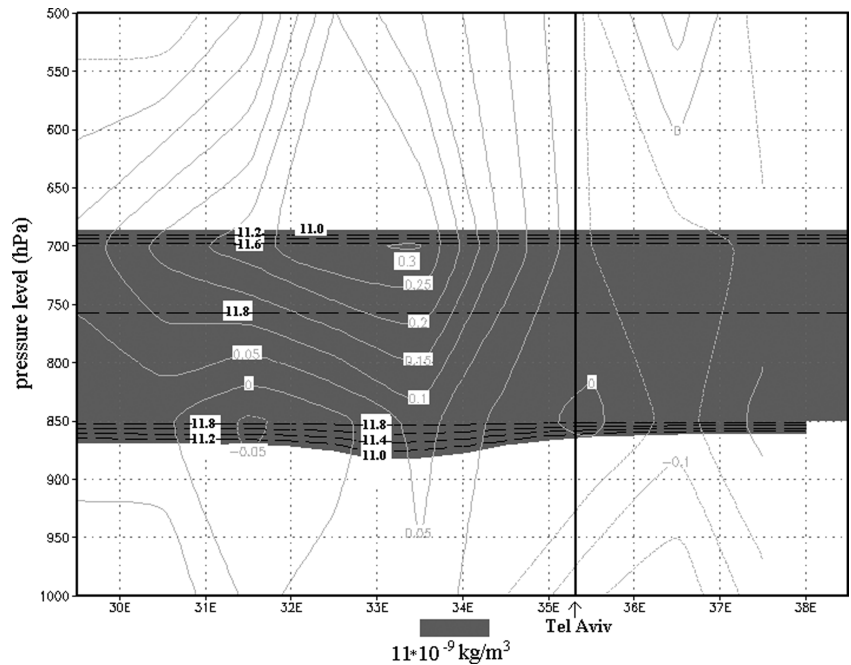


Fig. 5. The 32.5°N longitude cross-section of vertical profile (y-axis is pressure level in hPa) for the correlation between 700 hPa model temperature error  $\Delta T$  (K) at Tel Aviv (32.64°N, 35.28°E) and aerosol optical thickness (AOT) over the Eastern Mediterranean MODIS Terra gridpoints (see Section 2.1). The value of  $\Delta T$  is equal to (MM5 analysis 12 UTC) – (MM5 + forecast hours). Correlation for April 2001, 2002, 2004 & 2005 is for noon observations (12 UTC). Shaded areas are for  $\Delta T$  (+24) and black contour lines are for  $\Delta T$  (+12). The vertical bold line at longitude 35.28°E corresponds to the Tel Aviv model gridpoint.

4.3.3. *Back trajectories during a dust storm in Tel Aviv.* The mean westerly wind velocity during April for 32.5°N, 32.5°E at level 700 hPa is  $9 \text{ m s}^{-1}$  (for 2001–2004, NCEP reanalysis) or  $32 \text{ km h}^{-1}$ . This wind velocity corresponds to an air mass movement of 384 km in 12 h. Typical back trajectories of forecast time +48 h for April are shown for an extreme dust event in

Fig. 6. The 32.5°N latitudinal cross-section of vertical profile for ETA predicted maximum pressure levels of dust concentration ( $10^{-9} \text{ kg m}^{-3}$ , dashed contours and shaded area) of mineral aerosols at 12 UTC with a forecast time of +24 h, for April 2002–2005. Solid contour lines represent the correlation between Tel Aviv model temperature error (K) for +12 h and MODIS Terra aerosol optical thickness (AOT). Model temperature error is defined as (MM5 analysis 12 UTC) – (MM5 + forecast hours). The vertical bold line at longitude 35.28°E shows the Tel Aviv model gridpoint. The highest correlation (0.30) at longitude 33.5°E and pressure level 700 hPa is based on 60 observations. The number of observations, which the correlations are based on, is in the range of 54–91. Dust concentrations for levels 850, 700 and 500 hPa are based on 96–103 forecast cases. At level 1000, it is based on 95 forecast cases.



Tel Aviv. Back trajectories ended at the Tel Aviv gridpoint (32.0°N, 35°E) on 14 April 2005, 12 UTC. AOT measured by Terra on this typical day was 0.2. During the month of April, a typical source of aerosols is from North Africa as can be seen in Fig. 7. In Section 5.3, we explain why the lag correlation distance is only about 2° in longitude or approximately 200 km.

## 5. Discussion

### 5.1. Tel Aviv correlations between aerosols and model temperature errors

The negative sign of the correlation between high AOT ( $\text{AOT} \geq 0.5$ ) and UKMO  $\Delta T$  (+12 h) indicates a cooling effect, which is the result of interactions with aerosols. The majority of the cases in which AOT is equal to or greater than 0.5, are due to dust storms. In the data, there is an extreme AOT point,  $\text{AOT} = 1.1$ , for 16 April 2002. After excluding this extreme AOT datum from the correlation calculation, a negative correlation equal to  $-0.39$ , with a high significance level (2%) was still present. Linear regression exhibited a negative significant slope ( $p = 0.2\%$ ) equal to  $-4.2(\text{K}/\text{AOT})$ , with a standard deviation of  $1.2(\text{K}/\text{AOT})$ .

The aerosol layer in mineral dust storms has a high value of single scattering albedo in the visible spectrum. Therefore, reflected visible radiation by the aerosol layer is higher than absorbed radiation. Since most of the dust layer mass lies between 850 and 700 hPa and not lower (Fig. 1), in days with high AOT, most of the reflected radiation is higher than at 850 hPa. Consequently, less radiation reaches the ground from 850 hPa downward, causing a cooling effect in the lower layer.

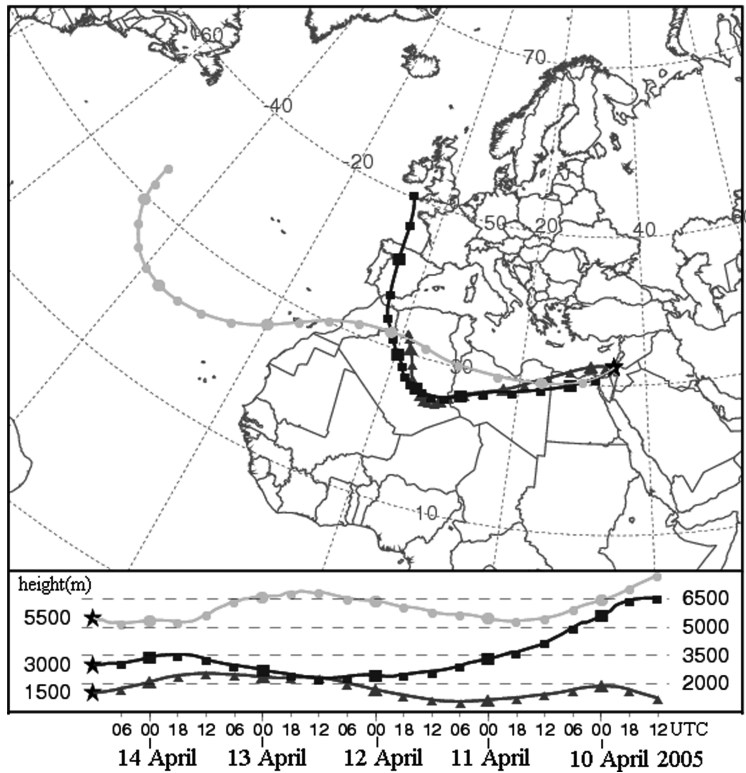


Fig. 7. Typical back trajectories of forecast time +48 h for the month of April. This typical back trajectory is for an extremely dusty day in Tel Aviv. Back trajectories end at Tel Aviv gridpoint 32.0°N, 35°E on 14 April 2005, 12 UTC. The line with triangles represents the height of 1500 m above ground level (agl), the line with squares is for the height of 3000 m agl and the line with circles is for the height of 5000 m agl (see Section 4.3.3). MODIS aerosol optical thickness (AOT) measured by Terra during this typical day was 0.2.

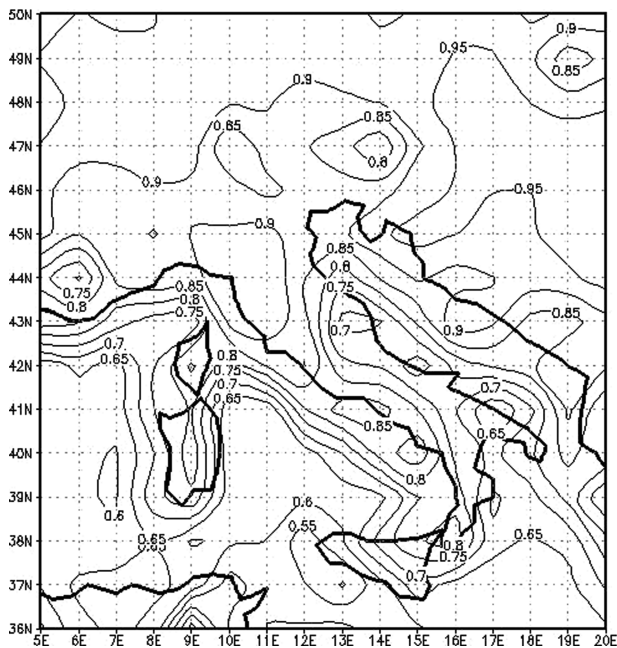


Fig. 8. The MODIS Terra aerosol optical thickness (AOT) fine mode fraction ( $f$ ) in Italy during January 2001–December 2001.

## 5.2. Italy results

In southern Italy  $f$  is lower than in central Italy, and drops down to 0.5 at 37°N, compared with 0.9 along the northern

border of the central zone. Figure 8 shows the distribution of  $f$  in Italy during the analysis period of January 2001–December 2001. This is explained by the fact that southern Italy is closer to the major dust source of North Africa (e.g. Barkan et al., 2005). As a result, southern Italy receives more mineral dust aerosols arriving from the Sahara. Additionally, in central Italy, the concentration of pollution is higher due to larger industries, which produce anthropogenic aerosols such as sulphate. High concentrations of industrial aerosols, which are often smaller in size than mineral dust aerosols, produce higher values of  $f$ , whereas high concentrations of coarse aerosols in the air, such as mineral dust, produce low values of  $f$ . Miller and Tegen (1998) showed that between June and August, dust that arrived from the desert can reduce surface air temperature by  $-0.4$  to  $-1.2$  K in the regions of Italy and Israel (NASA Science Briefs, 2007). This finding is in agreement with the values of the temperature reduction as induced from the temperature errors.

Sulphate and mineral dust aerosols produce high single scattering albedo in the visible spectrum. Kaufman et al. (2001) found that mineral dust aerosols have visible single scattering albedo ( $\omega$ ) equal to 0.97, with a standard deviation of 0.02. Sulphate aerosols have a visible  $\omega$  equal to 0.97 (Max-Planck Institute for Meteorology, 1997). However, in central Italy, aerosols also contain soot particles, which have a significantly lower  $\omega$  value, equal to about 0.62 (Max-Planck Institute for Meteorology, 1997), and other mixed aerosols of mineral dust, covered with sulphate on their surface. These, sulphate covered mineral dust aerosols have low  $\omega$  relative to clear mineral dust. The

visible single scattering albedo of mixed aerosols is less than 0.7. Hence, the average visible single scattering albedo is probably significantly lower in central Italy than in southern Italy. Low single scattering albedo is expressed by more radiation being absorbed than reflected.

This may explain why the correlation between surface  $\Delta T$  and AOT is positive in southern Italy and negative in central Italy. Similarly, Hansen and Nazarenko (2004) have shown that a critical value of global single scattering albedo for aerosols exists, which is of the order of 0.95–0.96. Above this value, the models show global cooling instead of global warming.

In Italy,  $\Delta T$  at ground level, and not at the 850 hPa level, was examined. Therefore, in some cases, the sign of correlation would be different from that in Tel Aviv. In central Italy, aerosol size is smaller than in southern Italy. Fine aerosols (radius mode less than  $1 \mu\text{m}$ ) interact more with electromagnetic radiation than coarse aerosols (radius mode greater than  $1 \mu\text{m}$ ). In southern Italy, however, the size of aerosols is in the  $2.5 \mu\text{m}$  radius mode, which interacts with near IR radiation. Therefore, in this area, more interaction between aerosols and IR or thermal ground radiation will be expected. In central Italy, the aerosols hardly interact with ground thermal radiation, and therefore, only direct solar radiation is reflected back causing ground cooling (negative correlation). In southern Italy, however, in addition to the reflection of direct solar radiation, there are also interactions between aerosols and thermal ground radiation, which can change the sign of correlation from negative to positive. If the effect of interactions between thermal ground radiation and aerosols on the air mass is strong enough compared with the direct solar effect, positive correlation (heating effect) will be measured. Thermal radiation can be reflected from the bottom of the dust layer back to the ground causing it to warm. In Tel Aviv, unlike in Italy, the 850 hPa level is above the bottom of the dust layer, and therefore, NIR warming due to the interaction with aerosols is lower compared with the cooling effect due to blocking of solar radiation by the aerosol layer. Satheesh et al. (2006) showed that mineral dust aerosols that are mixed with carbon absorb IR. The optical characteristics for coarse mineral shifted aerosols (size  $0.5 \mu\text{m}$ ) in ground thermal radiation ( $9.6 \mu\text{m}$ ) are: single scattering albedo 0.48, the asymmetry parameter ( $g$ ) 0.44 and the interaction coefficient  $0.026 \text{ m}^2 \text{ g}^{-1}$  (Max-Planck Institute for Meteorology, 1997). The above single scattering albedo value supports the argument that mineral dust in the infrared spectrum causes heating.

### 5.3. *The lag between maximum correlation in the Eastern Mediterranean and $\Delta T$ at the Tel Aviv gridpoint*

Correlation for  $\Delta T$  (+24 h) is expected to be less than that for the forecast time of +12 h because errors due to other factors in the model also increase with forecasting time. The effect of aerosols on the atmosphere is dominantly local, whereas at

larger forecast times, other effects, such as initial model data errors, model approximation errors and synoptic processes that the model does not compute exactly, all become more dominant.

In fact, the correlation obtained for  $\Delta T$  (+24 h) is higher than for  $\Delta T$  (+12 h), 0.34 and 0.30, respectively. A possible explanation for this is the low number of observations on which the correlations are based. For 60 observations and a correlation of 0.3, the interval confidence of 95% is 0.03. Therefore, it is possible that the difference between the correlations (0.34 and 0.30) is insignificant.

The distance that an air mass at 850 hPa should move in 12 h was calculated to be, in this case, 384 km (see Section 4.3.3). However, in Fig. 4 the distance between the maximum correlation for  $\Delta T$  (+24 h) and  $\Delta T$  (+12 h) is approximately 200 km.

There are a few reasons why the calculated lag distance for the averaged wind in April is almost double.

(1) The averaged wind ( $32 \text{ kmh}^{-1}$ ) that was used in the distance calculation, is for 700 hPa. The air mass started at a level lower than 700 hPa and during its journey, rose to 700 hPa. The average wind at a lower pressure level is smaller than that at 700 hPa; therefore, the distance lag should be reduced.

(2) The distance between every AOT gridpoint is about 100 km. This is not sensitive enough when compared with the obtained distance of 200 km. For this low resolution, a standard error of the order of tens of kilometres, in the measured lag distance is expected.

(3) Dusty days in April are typically caused by the North African Sharav low. Usually during these days, the southerly wind component is relatively high compared with other non-dusty days, and the westerly wind is relatively lower. This might be another reason why the lag distance is shorter than that calculated using average wind velocities.

## 6. Summary

The aim of this study was to try to identify and quantify the total atmospheric response to aerosols in numerical weather prediction models, through analysis of NWP model temperature errors.

Three significant findings are presented. First, the cooling effect at pressure level 850 hPa in the dust layer over the Tel Aviv area is caused by a high aerosol load (high AOT). This supports the hypothesis that cases of high aerosol mass influence model errors in a significant way. For lower AOT, other model or data problems such as initial conditions, misrepresentation of real microphysical processes, numerical errors and low grid resolution become more dominant than the aerosol effect. For high AOT, the effect of aerosols is stronger and therefore, model errors are more correlative with AOT. In addition, analysis of the correlation between AOT and different  $\Delta T$  forecast times, that is, 12, 24 and 36 h, indicates that the effect of aerosols on model errors is, as expected, stronger for shorter forecast

times. The effect of aerosols on model errors is more local than some of the other effects. For extended forecasting times, other model errors become dominant. Additionally, errors that develop with time, such as inaccurate initialization, increase with time, and errors caused by aerosols will then become inseparable from all other aforementioned errors. Analysis of  $\Delta T$  and AOT for Tel Aviv and Italy indicates that the situation is quite complex. The effect of aerosols depends not only on the value of AOT or the vertical integrated aerosol mass, but also on the vertical distribution of dust, the source and chemical composite of the aerosols, their size, life history, synoptic types and, finally, the very complex issue of aerosol-cloud interactions. The main conclusion, however, is that the total effect of aerosols on heating or cooling of the atmosphere can be quantified. Larger databases are expected to allow an even better definition of these effects. The aerosol-cloud interaction was not investigated here because observations and models lack reliable relevant atmospheric variables such as cloud amount, cloud type, droplet concentration with as a function of height, cloud top/base heights, etc.

In central Italy, for January 2001 to March 2002, correlation between ECMWF surface monthly  $\Delta T$  (+12 h) and MODIS Terra monthly AOT is negative ( $-0.72$ ) and is positive for southern Italy ( $+0.70$ ). Hence, in central Italy, the influence of aerosols on surface temperature is one of cooling, whereas over southern Italy, it is one of warming. To be more accurate about the influence of aerosols on temperature model errors ( $\Delta T$ ) there is a need to take into account additional factors in the analysis such as clouds and seasonal factors (or the solar radiation change).

The idea behind analysing correlations over the Eastern Mediterranean for April was that during this month, the frequency of dust storms is relatively higher. Another factor was to reduce the effect of seasonal changes on solar radiation. Examination of one month reduces the effect of changes in daily solar radiation because the daily solar radiation variation is small within a single month or within any specific season such as mid-summer.

Employing error observations over longer time periods will increase the significance of our findings. Another advantage is that a large number of observed AOT cases can help in dividing them into groups of high, medium and low AOT. This will refine our knowledge of the effect of aerosols as a function of AOT. Additionally, high AOT includes mainly one type of aerosol as opposed to low AOT. Grouping can assist in separating cases of different AOT types, and thereby, increase the understanding of not only how aerosols contribute to model errors but also how different types of aerosols contribute to these errors, as was demonstrated in Italy, on a monthly basis. However, including more months in the analysis will involve additional factors, such as average daily solar radiation, which varies greatly during the year, additional synoptic types, which change frequency during the year, and other seasonal factors. To isolate other factors

from aerosols, it is better to take large interval time slices or to examine only one month.

## 7. Acknowledgements

Our co-author, Dr. Yoram Kaufman (YK), NASA Goddard Space Flight Center, Maryland, USA, was very active in this study since 2001 while PA was on sabbatical at NASA. Actually, he suggested looking into NWP errors, and this study began at that time. YK lived to see an early version of this paper and nearly all the figures during our meeting in April 2006, just a few weeks before he was killed in a bicycle accident that occurred on 29 May 2006. This paper is dedicated to his memory. This research was partly supported by the GLOWA—Jordan River fund of the German Ministry of Science and Education (BMBF), in collaboration with the Israeli Ministry of Science and Technology (MOST) and by the EU-CIRCE project. This study was also supported by the Israeli Science Foundation (ISF grant No. 764/06). We acknowledge M. Colacino, CNR, Roma, who provided us with the data from Italy.

## References

- Alpert, P. and Ziv, B. 1989. The Sharav cyclone—observations and some theoretical considerations. *J. Geophys. Res.* **94**, 18 495–18 514.
- Alpert, P., Kaufman, Y. J., Shay-El, Y., Tanré, D., Da Silva, A. and co-authors. 1998. Quantification of dust-forced heating of the lower troposphere. *Nature* **395**, 367–370.
- Alpert, P., Herman, J., Kaufman, Y. J. and Carmona, I. 2000. Response of the climatic temperature to dust forcing, inferred from total ozone mapping spectrometer (TOMS) aerosol index and the NASA assimilation model. *J. Atmos. Res.* **53**, 3–14.
- Alpert, P., Krichak, S. O., Tsidulko, M., Shafir, H. and Joseph, J. H. 2002. A dust prediction system with TOMS initialization. *Mon. Wea. Rev.* **130**, 2335–2345.
- Alpert, P., Kishcha, P., Shtivelman, A., Krichak, S. O. and Joseph, J. H. 2004. Vertical distribution of Saharan dust based on 2.5-year model predictions. *Atmos. Res.* **70**, 109–130.
- Barkan, J., Alpert, P., Kutiel, H. and Kishcha, P. 2005. Synoptic of dust transportation days from Africa toward Italy and Central Europe. *J. Geophys. Res.* **110**, D06208.
- Buizza, R., Richardson, D. S. and Palmer, T. N. 2003. Benefits of increased resolution in the ECMWF ensemble system and comparison with poor-man's ensembles. *Q. J. R. Meteorol. Soc.* **129**, 1269–1288.
- ECMWF, 2002. Available at <http://www.ecmwf.int/research/predictability/projects/index.html>
- Erel, Y., Dayan, U., Rabi, R., Rudich, Y. and Stein, M. 2006. Trans boundary transport of pollutants by atmospheric mineral dust. *Environ. Sci. Technol.* **40**, 2996–3005.
- Hansen, J. and Nazarenko, L. 2004. Soot climate forcing via snow and ice albedos. *Proc. Natl. Acad. Sci.* **101**, 423–428.
- Intergovernmental Panel on Climate Change (IPCC), Climate change 2001. *The Scientific Basis*. Cambridge Univ. Press, Cambridge.
- Jacobson, M. Z. and Kaufman, Y. J. 2006. Wind reduction by aerosol particles. *Geophys. Res. Lett.* **33**, L24814.

- Kaufman, Y. J., Tanré, D., Dubovik, O., Karnieli, A. and Remer, L. A. 2001. Absorption of sunlight by dust as inferred from satellite and ground-based remote sensing. *Geophys. Res. Lett.* **28**, 1479–1482.
- Kaufman, Y. J., Tanré, D. and Boucher, O. 2002. A satellite view of aerosols in climate system. *Nature* **419**, 215–223.
- Krichak, S. O., Alpert, P. and Dayan, M. 2007. A Southeastern Mediterranean PV streamer and its role in December 2001 case with torrential rains in Israel. *Nat. Hazards Earth Syst. Sci.* **7**, 21–32.
- Max-Planck Institute for Meteorology, Hamburg, Germany 1997. Global Aerosol Data Set, Report 243.
- Miller, R. L. and Tegen, I. 1998. Climate response to soil dust aerosols. *J. Climate* **11**, 3247–3267.
- MODIS, 2007a. Available at [http://g0dup05u.ecs.nasa.gov/Giovanni/modis.MOD08\\_M3.shtml](http://g0dup05u.ecs.nasa.gov/Giovanni/modis.MOD08_M3.shtml).
- MODIS, 2007b. Available at [http://g0dup05u.ecs.nasa.gov/Giovanni/modis.MOD08\\_D3.shtml](http://g0dup05u.ecs.nasa.gov/Giovanni/modis.MOD08_D3.shtml).
- NASA Science Briefs, 2007. Available at [http://www.giss.nasa.gov/research/briefs/miller\\_01/](http://www.giss.nasa.gov/research/briefs/miller_01/).
- Ramanathan, V., Crutzen, P. J., Kiehl, J. T. and Rosenfeld, D. 2001. Aerosols, climate, and the hydrological cycle. *Science* **294**, 2119–2124.
- Satheesh, S.K., Deepshikha, S., Srinivasan, J. and Kaufman, Y. J. 2006. Large dust absorption of infrared radiation over Afro-Asian regions: evidence for anthropogenic impact. *IEEE Geosci. Remote Sens. Lett.* **111**, D08202.
- Tanré, D., Kaufman, Y. J., Holben, B. N., Chatenet, B., Karnieli, A., and co-authors. 2001. Climatology of dust aerosol size distribution and optical properties derived from remotely sensed data in the solar spectrum. *J. Geophys. Res.* **106**, 18 205–18 217.
- TAU-WERC, 2007. Available at <ftp://ftp.nasa.proj.ac.il/mm5/current/mm5.html>.
- Wanger, A., Peleg, M., Sharf, G., Mahrer, Y., Dayan, U., and co-authors. 2000. Some observational and modeling evidence of long-range transport of air pollutants from Europe toward Israeli coast. *J. Geophys. Res.* **105**, 7177–7186.
- Xiong X., Sun, J., Esposito, J., Guenther, B. and Barnes, W. L. 2003. MODIS reflective solar bands calibration algorithm and on-orbit performance. In: *Proceedings of SPIE—Optical Remote Sensing of the Atmosphere and Clouds III*. **4891**, 95–104.